



ORIGINAL RESEARCH ARTICLE

[^{99m}Tc]Tc-HYNIC-Octreotide scintigraphy in melanoma: A preliminary report

Ehsan Soltani¹, Sajjad Sadeghpour², Ehsan Hasanzadeh Hadad¹, Faezeh Rabbani Banoo², Hanieh Elahifard², Vahid Roshanravan², Maryam Emadzadeh³, Salman Soltani⁴, Kamran Aryana², Nasrin Raeisi², Farzane Akbari², Nahid Jalalian Elahi², Maryam Zoghi², Ramin Sadeghi², Kayvan Sadri², Kazem Anvari⁵, Zahra Bakhshi², Atena Aghae²

¹Oncosurgery Research Center, Mashhad University of Medical Sciences, Mashhad, Iran

²Nuclear Medicine Research Center, Mashhad University of Medical Sciences, Mashhad, Iran

³Clinical Research Development Unit, Ghaem Hospital, Mashhad University of Medical Sciences, Mashhad, Iran

⁴Kidney Transplantation Research Center, Mashhad University of Medical Sciences, Mashhad, Iran

⁵Cancer Research Center, Mashhad University of Medical Sciences, Mashhad, Iran

ARTICLE INFO

Article History:

Received: 30 October 2025

Revised: 22 January 2026

Accepted: 25 January 2026

Published Online: 22 June 2026

Keyword:

Melanoma

[^{99m}Tc]Tc-HYNIC-Octreotide

Scintigraphy

[¹⁷⁷Lu]Lu-DOTATATE

***Corresponding Author:**

Dr. Atena Aghae

Address: Nuclear Medicine Research Center, Mashhad University of Medical Sciences (MUMS), Mashhad, Khorasan Razavi, Iran

Email: aghaeat@gmail.com

ABSTRACT

Introduction: This study aimed to evaluate the expression of SSTRs in metastatic melanoma lesions using [^{99m}Tc]Tc-HYNIC-Octreotide whole-body scintigraphy and SPECT/CT imaging, and to assess its potential role in identifying candidates for receptor-targeted therapies such as peptide receptor radionuclide therapy (PRRT) with [¹⁷⁷Lu]Lu-DOTATATE.

Methods: Eight patients with suspected or confirmed melanoma underwent [^{99m}Tc]Tc-HYNIC-Octreotide imaging. Imaging findings were assessed visually using Krenning scores and quantitatively via lesion-to-liver uptake ratios. Histopathology served as the reference standard.

Results: Among seven histologically confirmed melanoma cases, six demonstrated radiotracer uptakes on SPECT/CT, though only four met the threshold for a positive scan (Krenning score ≥ 2). These four were classified as true positives, while the remaining three were false negatives. Quantitative analysis revealed that true-positive lesions had a significantly higher mean lesion-to-liver uptake ratio than false negatives (1.22 vs. 0.28; $p = 0.009$).

Conclusion: [^{99m}Tc]Tc-HYNIC-Octreotide scintigraphy demonstrates potential as a non-invasive tool for assessing SSTR expression in metastatic melanoma. This imaging approach may help identify patients who could benefit from SSTR-targeted therapies, particularly those unresponsive to conventional treatment. Further large-scale studies are warranted to validate these findings and explore the role of SSTR imaging in personalized melanoma management.

Use your device to scan and read the article online



How to cite this article: Soltani E, Sadeghpour S, Hasanzadeh Hadad E, Rabbani Banoo F, Elahifard H, Roshanravan V, Emadzadeh M, Soltani S, Aryana K, Raeisi N, Akbari F, Jalalian Elahi N, Zoghi M, Sadeghi R, Sadri K, Anvari K, Bakhshi Z, Aghae A. [^{99m}Tc]Tc-HYNIC-Octreotide scintigraphy in melanoma: A preliminary report. Iran J Nucl Med. 2026;34(2):113-119.



<https://doi.org/10.22034/irjnm.2026.130362.1718>

INTRODUCTION

Skin cancer, particularly non-melanoma types, is among the most commonly diagnosed cancers worldwide. Cutaneous melanoma (CM), although less prevalent, is its most aggressive and lethal subtype and accounts for the majority of skin cancer-related deaths. In some populations, CM ranks among the most common cancers in adults, particularly in fair-skinned individuals living in high UV exposure regions [1-3]. It arises from melanocytes, neural crest-derived pigment-producing cells that play a vital role in photoprotection through melanin production. Despite increased awareness and improvements in early detection, the global burden of CM remains high, with approximately 132,000 new diagnoses annually [4-6]. Melanoma staging, based on tumor thickness (Breslow score), nodal involvement, and metastasis, categorizes disease into four stages. While stages I and II signify localized disease and are often curable via surgical excision, stages III and IV involve regional and distant metastasis and are associated with poorer prognoses. The therapeutic landscape of advanced melanoma (AM) has transformed over the past decade, largely due to immunotherapies (e.g., anti-PD-1, anti-CTLA-4) and targeted agents (e.g., BRAF and MEK inhibitors). However, resistance and recurrence remain common, necessitating alternative diagnostic and therapeutic approaches [5]. Somatostatin and its analogues (SSAs) bind to somatostatin receptors (SSTRs) 1–5 with varying affinities. These compounds directly inhibit cell growth by modulating cell proliferation and inducing apoptosis. Several studies have highlighted that SSAs exhibit antitumor effects by interacting with SSTRs across various tumor types, including those originating from the pituitary, prostate, gastric, lung, pancreatic, colorectal, and thyroid tissues [7-10]. The expression of SSTRs has been notably observed in human melanoma tissues and melanoma cell lines [11, 12]. However, some studies have recently challenged the concept of the therapeutic effect of SSAs in AM, demonstrating that SSAs did not significantly inhibit melanoma evolution [13]. The expression of SSTRs in CM can be leveraged for therapeutic purposes by using novel radiolabeled SSAs, which can potentially target receptor-expressing cells selectively. Radiotheranostic SSAs have been extensively utilized in the treatment of human neuroendocrine tumors (NETs). Due to the elevated levels of SSTRs in these tumors, this therapeutic approach has demonstrated positive outcomes in reducing tumor growth and improving patient survival [14]. The success of SST-targeted peptide-based agents in NETs has paved the way for investigating their therapeutic effects in other SSTR-positive tumors. The expression of SSTRs in CM was

assessed for potential therapeutic applications in a small-scale study in 2001 by Lum et al. This study indicated that SSTR2 expression on a ¹¹¹In-pentetreotide octreoscan can be transcribed into a functional protein that could be utilized as a diagnostic tool on an octreoscan [11]. If SSTR is sufficiently expressed in cases of AM that are resistant to conventional therapies, targeting SSTR with agents such as [¹⁷⁷Lu]Lu-DOTATATE may represent a promising therapeutic option [15]. Although extensive research has been carried out on evaluating SSTR expression in various tumors, much less is known about CM. [^{99m}Tc]Tc-HYNIC-Octreotide, a radiopharmaceutical that selectively binds to somatostatin receptors, has emerged as a non-invasive imaging modality for evaluating SSTR expression in tumors. This agent allows for whole-body imaging, providing valuable insights into the functional status of SSTRs in metastatic lesions and is particularly advantageous as it may facilitate the identification of patients who are likely to benefit from radiolabeled SSA therapy [16, 17]. The present study attempts to evaluate the functional status of SSTR expression in metastatic melanoma lesions utilizing [^{99m}Tc]Tc-HYNIC-Octreotide whole-body imaging and to validate the clinical utility of this diagnostic approach. Additionally, understanding the patterns of SSTR expression may have significant implications for therapeutic decision-making and the personalization of treatment protocols in CM management, including peptide receptor radionuclide therapy (PRRT) with [¹⁷⁷Lu]Lu-DOTATATE. Through this investigation, we seek to contribute to the advancing landscape of melanoma diagnosis and treatment, ultimately enhancing patient care in this complex disease.

METHODS

Eight patients with clinically suspected or histologically confirmed melanoma were referred for [^{99m}Tc]Tc-HYNIC-Octreotide whole-body scintigraphy with additional SPECT/CT imaging before surgery at our nuclear medicine department. All participants were thoroughly informed about the imaging protocol and potential additional procedures for research purposes. This study was approved by the Ethics Committee of Mashhad University of Medical Sciences (Ethics code: IR.MUMS.MEDICAL.REC.1400.03).

Two patients had a prior history of primary tumor resection in the lower extremity and were re-evaluated for suspected inguinal lymph node metastases. The remaining patients were either biopsy-proven or clinically highly suspicious for melanoma. All patients underwent surgical excision of suspected lesions or biopsy, and histopathologic

examination was performed as the reference standard.

Experienced nuclear medicine physicians reviewed all [^{99m}Tc]Tc-HYNIC-Octreotide scans. The following imaging parameters were recorded for each patient: physiological and abnormal uptake patterns, location and size of suspicious lesions, maximum radiotracer uptake in lesions, mean liver uptake, Krenning score (0–4 scale), and lesion-to-liver uptake ratio (calculated as maximum lesion count divided by mean liver count).

Quantitative analysis was performed using axial SPECT/CT fusion images. Volumes of interest (VOIs) were drawn over the tumor and liver. The lesion's maximum and the liver's mean uptake were used to compute the lesion-to-liver uptake ratio, which was subsequently compared with histopathologic results.

[^{99m}Tc]Tc-HYNIC-Octreotide SPECT/CT protocol

Four hours after intravenous administration of 740 MBq (20 mCi) of [^{99m}Tc] Tc-HYNIC-Octreotide, whole-body planar scintigraphy was performed using a dual-head gamma camera (GE) equipped with low-energy high-resolution (LEHR) collimators. Imaging parameters were: 12 cm/min bed speed, matrix size 256×1024, and a 140 keV photopeak with a 10% energy window. SPECT acquisition was followed using a 128×128 matrix, 64 projections in a non-circular orbit, and 20 seconds per step. Images were reconstructed with ordered-subset expectation maximization (OSEM; 8 iterations, 4 subsets). Low-dose CT was acquired for attenuation correction and anatomical correlation (spatial resolution 3 mm, 120 kV, 60–80 mAs).

Statistical analysis

Descriptive statistics were used to summarize demographic and clinical characteristics. Scans were considered positive when the lesion demonstrated a Krenning score ≥ 2 . Quantitative comparison of lesion-to-liver uptake ratios between true-positive and false-negative groups was performed using the Mann–Whitney U and Welch's t-test, depending on the distribution and sample size considerations. The association between scan positivity (Krenning ≥ 2) and histopathologic confirmation was further evaluated using Fisher's exact test. A two-sided p-value < 0.05 was considered statistically significant. All statistical analyses were conducted using SPSS software, version 26.

RESULTS

Patient demographics and clinical characteristics are summarized in Table 1. The mean age was 69.5 \pm 11.60 years, and 4 patients (50%) were male. Two patients presented with metastatic melanoma of

unknown primary origin—one involving the submental region (Figure 1) and the other located in the jejunum. Two additional patients had a prior history of lower extremity melanoma resection and were referred for evaluation of suspected inguinal lymph node metastases. Three other patients had biopsy-confirmed primary melanoma and subsequently underwent resection of the primary tumor, with or without regional lymph node dissection. One patient with a suspicious foot lesion underwent biopsy, which revealed no evidence of melanoma; this case was excluded from further analysis.

Table 1. Descriptive features

Total patients (n)		8
Gender, n (%)	Male	4 (50%)
	Female	4 (50%)
Primary tumor site, n (%)	Lower extremity	4 (50%)
	Scalp (occipital)	1 (12.5%)
	Esophagus	1 (12.5%)
	Unknown	2 (25%)
Surgical history, n (%)	No prior surgery	5 (62.5%)
	Prior surgery	3 (37.5%)

Visual assessment of [^{99m}Tc]Tc-HYNIC-Octreotide SPECT/CT demonstrated at least mild radiotracer uptake (Krenning score ≥ 1) in 6 of 7 histopathologically confirmed melanoma lesions (Figure 2), with varying contrast relative to physiological uptake in the liver and other organs. Of these, 4 lesions were classified as true positives and 3 as false negatives (Table 2). In all true-positive cases, focal tracer accumulation corresponded anatomically with suspicious findings on SPECT/CT and was subsequently confirmed by histopathologic analysis.

Quantitative evaluation showed that the mean lesion-to-liver uptake ratio was higher in true-positive cases compared to false-negative cases (1.22 vs. 0.28, respectively). While the Mann–Whitney U test did not reach statistical significance (although so close, $p = 0.057$), indicating that higher uptake ratios were not associated with histopathologic confirmation.

The association between scan results and final histopathologic findings was further assessed using Fisher's exact test, which yielded a p-value of 1.00, indicating no statistically significant relationship in this limited cohort.

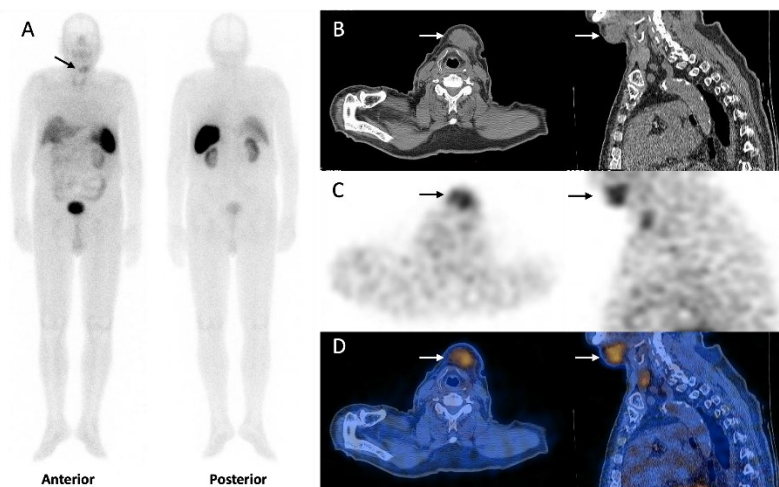


Figure 1. [^{99m}Tc]Tc-HYNIC-Octreotide SPECT/CT images of an 89-year-old man (Case 1) with metastatic melanoma of unknown primary origin. Moderate radiotracer uptake (arrows) is observed in a left submental soft tissue mass (Krenning score 2), corresponding anatomically to the lesion on CT. Histopathologic examination confirmed metastatic melanoma

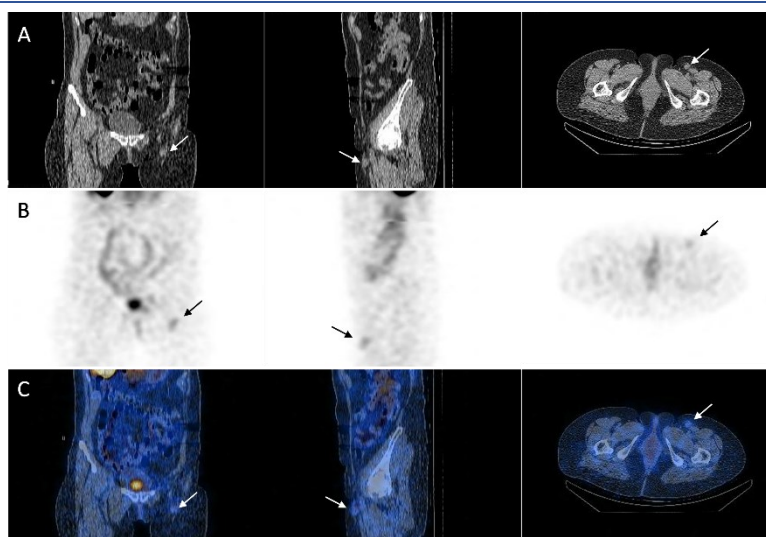


Figure 2. [^{99m}Tc]Tc-HYNIC-Octreotide SPECT/CT images of a 55-year-old woman (Case 2) with a prior history of primary melanoma in the lower extremity. Mild radiotracer uptake (arrows) is observed in a left inguinal lymph node (Krenning score 1), which corresponded histopathologically to a metastatic lymph node

DISCUSSION

Clinical context and importance of SSTRs in melanoma

The present study was designed to evaluate the diagnostic imaging of cutaneous melanoma (CM), particularly in assessing somatostatin receptor (SSTR) expression in metastatic melanoma lesions utilizing [^{99m}Tc]Tc-HYNIC-Octreotide whole-body imaging. This study is particularly relevant given the increasing incidence of CM and the challenges associated with managing advanced melanoma (AM), which remains a leading cause of cancer-related mortality. The expression of SSTRs in melanoma tissues has been documented [11, 12],

suggesting a potential therapeutic target for somatostatin analogs (SSAs). While SSAs have shown promise in various tumor types, their efficacy in melanoma has been debated, with some studies indicating limited impact on tumor progression [13]. The current study investigates the ability to visualize SSTR expression through non-invasive imaging techniques like [^{99m}Tc]Tc-HYNIC-Octreotide scintigraphy, providing critical insights into the functional status of these receptors in melanoma, potentially guiding therapeutic decisions. The apparent mismatch between visual positivity, Krenning-based readout, and semiquantitative lesion-to-liver ratios in our cohort

is biologically plausible and, in melanoma, likely reflects SSTR heterogeneity rather than a purely measurement problem. Visual reads integrate pattern, focality, and anatomic concordance on SPECT/CT, so a small, sharply focal deposit can be called positive even when its averaged or peak-derived ratio is only modest, especially near organs with high physiologic activity. By contrast, a lesion-to-liver ratio is sensitive to technical and biological confounders, such as partial-volume effects in small nodes, motion/misregistration, ROI placement, and variable liver reference uptake, which can compress ratios toward unity or below despite visually convincing focal uptake. Modern work in SSTR SPECT/CT underscores that visual Krenning scoring and quantitative metrics correlate only imperfectly, and that quantification can improve consistency but does not eliminate discordance, particularly in low-contrast or small-

volume disease. Clinically, these matters because melanoma lesions may express SSTRs patchily and variably between patients and even between lesions in the same patient, meaning that a visually positive focus with a borderline ratio may still represent a true SSTR-expressing clone, while visually mild uptake with a low ratio may represent either low receptor density or a non-SSTR-dominant biology. Practically, our findings argue for interpreting [^{99m}Tc]Tc-HYNIC-Octreotide as a phenotypic marker of receptor expression rather than a strictly intensity-threshold test, and they suggest that discordant visual/quantitative results should prompt careful correlation with lesion size, location, and histopathology, because receptor heterogeneity could influence both detection sensitivity and any future consideration of receptor-targeted strategies.

Table 2. Detailed [^{99m}Tc]Tc-HYNIC-Octreotide scintigraphy and histopathology patient data

No.	Age/Sex	Lesion Site	Site of uptake	Lesion-to-Liver uptake ratio*	Krenning Score	Histopathology	Classification
1	89/M	Submental mass	Submental mass	1.15	2	Metastatic melanoma	TP
2	55/F	Inguinal LN	Inguinal LN	0.55	1	Metastatic melanoma	FN
3	75/M	Inguinal LN	Inguinal LN	1.37	2	Metastatic melanoma	TP
4	62/F	Esophageal lesion	None	0.00	0	Malignant melanoma	FN
5	78/M	Occipital lesion	Occipital lesion	1.47	3	Malignant melanoma	TP
6	75/M	Foot + inguinal LNs	Inguinal LNs	0.29	1	Primary melanoma and nodal metastasis	FN
7	64/F	Jejunum	Jejunum	0.90	2	Metastatic melanoma	TP
8	58/F	Foot	None	0.00	0	Negative (no melanoma detected)	-

*Uptake Ratio = Max Lesion Uptake / Mean Liver Uptake

TP = True Positive; FN = False Negative

Methodological considerations

The study involved a small cohort of eight patients, limiting the findings' generalizability. However, the rigorous methodology, including the use of SPECT/CT imaging and histopathological correlation, strengthens the validity of the results. The imaging protocol employed was well-defined, focusing on quantifying radiotracer uptake through lesion-to-liver uptake ratios and Krenning scores.

These parameters are crucial for assessing the diagnostic accuracy of the imaging modality.

Clinical implications of imaging findings

Somatostatin receptors, particularly subtypes SSTR2 and SSTR3, have been implicated in various malignancies, including CM, where they may influence tumor proliferation, apoptosis, and metastatic behavior [18-20]. In this study, radiotracer uptake was observed in most

histologically confirmed melanoma lesions, though not all reached the positivity threshold based on Krenning scores. This variation suggests heterogeneity in SSTR expression among metastatic lesions, highlighting the need for receptor-specific imaging as a complementary modality to standard anatomical and metabolic imaging. These observations are consistent with prior studies indicating a possible role for SSTRs in melanoma pathophysiology [11, 21, 22]. However, there remains limited data in the literature on quantifying SSTR expression via non-invasive imaging techniques. Despite this gap, such approaches hold clinical value by supporting personalized treatment planning and patient stratification. This is especially pertinent as interest grows in SSTR-targeted therapies, including peptide receptor radionuclide therapy (PRRT) with agents like [¹⁷⁷Lu]Lu-DOTATATE [23]. Moreover, our study underscores the potential of [^{99m}Tc]Tc-HYNIC-Octreotide imaging as a complementary tool to conventional imaging modalities such as PET and CT scans. While PET imaging with 18F-FDG is widely used for assessing metabolic activity in tumors, it does not provide specific information regarding receptor expression. In contrast, [^{99m}Tc]Tc-HYNIC-Octreotide targets SSTRs, offering a more comprehensive understanding of tumor biology and heterogeneity [24]. This may enhance the detection of lesions that are not metabolically active but still express SSTRs, which could be crucial for treatment planning. The mean Krenning score of 1.4 ± 1.2 observed in our study is comparable with similar investigations in neuroendocrine tumors and supports its application in evaluating melanoma lesions [25]. Although the observed Krenning scores in this study are numerically similar to those reported in neuroendocrine tumors (NETs), it should be clarified that Krenning scoring thresholds were originally developed for NETs and may not be directly applicable to melanoma without further validation. While prior work has linked SSTR expression with treatment responsiveness in other malignancies, more data are needed to determine whether SSTR density in melanoma correlates with tumor aggressiveness or therapeutic outcomes [26].

Clinical significance and future directions

As complementary immunohistochemical analyses revealed strong receptor expression in tumor samples with high uptake values, the potential for combined imaging and therapeutic strategies emerges. As the landscape of melanoma treatment continues to evolve with the advent of immunotherapies and targeted therapies, integrating novel imaging modalities like [^{99m}Tc]Tc-

HYNIC-Octreotide scintigraphy could play a key role in optimizing patient management. Clinical trials are investigating various SSTR-targeted therapies that could benefit patients with high receptor expression, as identified through imaging studies. Future studies should establish standardized protocols incorporating [^{99m}Tc]-HYNIC-Octreotide imaging as a diagnostic tool for selecting suitable candidates for SSA therapies and PRRT with [¹⁷⁷Lu]Lu-DOTATATE. Moreover, expanding the imaging scope to include longitudinal assessments could provide insights into changes in receptor expression during treatment, thereby contributing to personalized therapy in melanoma care.

Limitations

While the study provides valuable findings, its limitations must be acknowledged. While adequate for preliminary analysis, the sample size remains limited, which may limit the generalizability of the results. Furthermore, variations in lesion characteristics and patient demographics could influence SSTR expression and imaging uptake patterns. Another important point to highlight is the limited applicability of the [^{99m}Tc]-HYNIC-Octreotide imaging in localizing the lesions that can be diffed more in future studies. Future studies with larger cohorts and diverse populations are necessary to validate these findings and assess the reproducibility of the results. Additionally, exploring the relationship between SSTR expression and treatment response in a longitudinal manner could provide further evidence for the therapeutic utility of SSAs in CM.

CONCLUSION

The preliminary report on [^{99m}Tc]Tc-HYNIC-Octreotide whole-body scintigraphy in CM scintigraphy shows potential as a non-invasive tool for assessing SSTR expression in metastatic melanoma. By leveraging the functional status of SSTR expression, this imaging modality may facilitate personalized treatment approaches, ultimately improving patient care in the complex management of AM. This imaging approach may help identify patients who could benefit from SSTR-targeted therapies, particularly those unresponsive to conventional treatment. Further research in this area is needed to establish the clinical utility of SSTR imaging in routine practice and its potential role in improving outcomes for patients with CM.

REFERENCES

1. Aggarwal P, Knabel P, Fleischer AB Jr. United States burden of melanoma and non-melanoma skin cancer from 1990 to 2019. *J Am Acad Dermatol.* 2021 Aug;85(2):388-95.

2. Jenkins RW, Fisher DE. Treatment of advanced melanoma in 2020 and beyond. *J Invest Dermatol*. 2021 Jan;141(1):23-31.
3. Ferdosi S, Saffari M, Eskandarieh S, Raziye R, Moghaddam MG, Ghanadan A, Shirkoohi R. Melanoma in Iran: a retrospective 10-year study. *Asian Pac J Cancer Prev*. 2016;17(6):2751-5.
4. Roky AH, Islam MM, Ahasan AMF, Mostaq MS, Mahmud MZ, Amin MN, Mahmud MA. Overview of skin cancer types and prevalence rates across continents. *Cancer Pathog Ther*. 2024 Aug 8;3(2):89-100.
5. Villani A, Potestio L, Fabbrocini G, Troncone G, Malapelle U, Scalvenzi M. The treatment of advanced melanoma: therapeutic update. *Int J Mol Sci*. 2022 Jun 7;23(12):6388.
6. Ahmadi F, Karamitanha F, Ramezanzpour A. Clustering trends of melanoma incidence and mortality: a worldwide assessment from 1995 to 2019. *Australas J Dermatol*. 2022 Aug;63(3):e206-17.
7. González-Barcena D, Schally AV, Vadillo-Buenfil M, Cortez-Morales A, Hernández L V, Cardenas-Cornejo I, Comaru-Schally AM. Response of patients with advanced prostatic cancer to administration of somatostatin analog RC-160 (vapeptide) at the time of relapse. *Prostate*. 2003 Aug 1;56(3):183-91.
8. Heaney AP, Melmed S. Molecular targets in pituitary tumours. *Nat Rev Cancer*. 2004 Apr;4(4):285-95.
9. Schally AV, Szepeshazi K, Nagy A, Comaru-Schally AM, Halmos G. New approaches to therapy of cancers of the stomach, colon and pancreas based on peptide analogs. *Cell Mol Life Sci*. 2004 May;61(9):1042-68.
10. Sidéris L, Dubé P, Rinke A. Antitumor effects of somatostatin analogs in neuroendocrine tumors. *Oncologist*. 2012;17(6):747-55.
11. Lum SS, Fletcher WS, O'Dorisio MS, Nance RW, Pommier RF, Caprara M. Distribution and functional significance of somatostatin receptors in malignant melanoma. *World J Surg*. 2001 Apr;25(4):407-12.
12. Dummer R, Michielin O, Nägeli MC, Goldinger SM, Campigotto F, Kriemler-Krahn U, Schmid H, Pedroncelli A, Micalletto S, Schadendorf D. Phase I, open-label study of pasireotide in patients with *BRAF*-wild type and *NRAS*-wild type, unresectable and/or metastatic melanoma. *ESMO Open*. 2018 Jul 23;3(5):e000388.
13. Scheau C, Draghici C, Ilie MA, Lupu M, Solomon I, Tampa M, Georgescu SR, Caruntu A, Constantin C, Neagu M, Caruntu C. Neuroendocrine factors in melanoma pathogenesis. *Cancers (Basel)*. 2021 May 10;13(9):2277.
14. Chambers C, Chitwood B, Smith CJ, Miao Y. Elevating theranostics: The emergence and promise of radiopharmaceutical cell-targeting heterodimers in human cancers. *iRadiology*. 2024 Apr;2(2):128-55.
15. Priyadarshini S, Allison DB, Chauhan A. Comprehensive assessment of somatostatin receptors in various neoplasms: a systematic review. *Pharmaceutics*. 2022 Jul 1;14(7):1394.
16. Kıraç S. Fundamentals of radiation safety and dosimetric approach in radionuclide therapy applications. In: Bekiş R, Polack B, Bozkurt MF, editors. *Radionuclide therapy*. Cham: Springer; 2022. p. 29–62.
17. Stojanovic B, Gajovic N, Jurisevic M, Stojanovic MD, Jovanovic M, Jovanovic I, Stojanovic BS, Milosevic B. Decoding the IL-33/ST2 axis: its impact on the immune landscape of breast cancer. *Int J Mol Sci*. 2023 Sep 13;24(18):14026.
18. Kumar U. Somatostatin and somatostatin receptors in tumour biology. *Int J Mol Sci*. 2023 Dec 28;25(1):436.
19. Kasprzak A, Geltz A. The state-of-the-art mechanisms and antitumor effects of somatostatin in colorectal cancer: a review. *Biomedicines*. 2024 Mar 5;12(3):578.
20. Bodei L, Kidd MS, Singh A, van der Zwan WA, Severi S, Drozdov IA, Cwikla J, Baum RP, Kwekkeboom DJ, Paganelli G, Krenning EP, Modlin IM. PRRT genomic signature in blood for prediction of ¹⁷⁷Lu-octreotate efficacy. *Eur J Nucl Med Mol Imaging*. 2018 Jul;45(7):1155-69.
21. Valencak J, Heere-Ress E, Traub-Weidinger T, Raderer M, Schneeberger A, Thalhammer T, Aust S, Hamilton G, Virgolini I, Pehamberger H. Somatostatin receptor scintigraphy with ¹¹¹In-DOTA-lanreotide and ¹¹¹In-DOTA-Tyr3-octreotide in patients with stage IV melanoma: in-vitro and in-vivo results. *Melanoma Res*. 2005 Dec;15(6):523-9.
22. Bodei L, Kwekkeboom DJ, Kidd M, Modlin IM, Krenning EP. Radiolabeled somatostatin analogue therapy of gastroenteropancreatic cancer. *Semin Nucl Med*. 2016 May;46(3):225-38.
23. Bozkurt MF, Virgolini I, Balogova S, Beheshti M, Rubello D, Decristoforo C, Ambrosini V, Kjaer A, Delgado-Bolton R, Kunikowska J, Oyen WJG, Chiti A, Giammarile F, Sundin A, Fanti S. Guideline for PET/CT imaging of neuroendocrine neoplasms with ⁶⁸Ga-DOTA-conjugated somatostatin receptor targeting peptides and ¹⁸F-DOPA. *Eur J Nucl Med Mol Imaging*. 2017 Aug;44(9):1588-601.
24. Kim JY, Kim J, Kim YI, Yang DH, Yoo C, Park IJ, Ryoo BY, Ryu JS, Hong SM. Somatostatin receptor 2 (SSTR2) expression is associated with better clinical outcome and prognosis in rectal neuroendocrine tumors. *Sci Rep*. 2024 Feb 19;14(1):4047.
25. Ardjomand N, Ardjomand N, Schaffler G, Radner H, El-Shabrawi Y. Somatostatin receptor expression in uveal melanomas. *Invest Ophthalmol Vis Sci*. 2003 Mar;44(3):980-7.